Selective reduction of NO_2 with acetaldehyde over Co/Al_2O_3 in lean conditions

Atsushi Takahashi*, Masaaki Haneda,
Tadahiro Fujitani, Hideaki Hamada

*Research Institute for Innovation in Sustainable Chemistry, National Institute of Advanced Industrial
Science and Technology (AIST), Tsukuba Central 5, 1-1-1 Higashi, Tsukuba, Ibaraki 305-8565, Japan*

Abstract

Selective reduction of NO_2 with acetaldehyde (CH_3CHO) was investigated over alumina-supported catalysts. Among the catalysts tested, Co/Al_2O_3 showed the highest activity with a maximum performance at 2 wt.% Co loading. The comparison of the activity of Co/Al_2O_3 and Al_2O_3 for several unit reactions suggested that one of the roles of supported Co is to suppress the combustion of CH_3CHO by O_2, resulting in an enhancement of the selective reaction of CH_3CHO with NO_2. The observation of the adsorbed species by in situ FT-IR spectroscopy showed that enolate species acts as the intermediate for NO_2 reduction by CH_3CHO and that another role of Co is to promote the production of the enolate species.
© 2006 Elsevier B.V. All rights reserved.

Keywords: Acetaldehyde; Co/Al_2O_3; NO_2 selective reduction

1. Introduction

Selective catalytic reduction of nitrogen oxide (NOx) with hydrocarbon (HC-SCR) is one of the most desirable technologies for abatement of NOx in diesel and lean burn engine exhausts. While a lot of investigations have focused on zeolite-based catalysts since the report on Cu–ZSM-5 catalyst by Held et al. [1] and Iwamoto et al. [2], metal oxide-based catalysts represented by alumina have also drawn considerable attention [3–5].

The selective reduction of NO with hydrocarbon is a very complex reaction comprised of several parallel and/or consecutive reaction steps. Although there is still disagreement in the literature regarding the reaction pathway, this reaction is believed to be a three-step process consisting of: (I) NO oxidation to NO_2, (II) oxidative activation of hydrocarbon, and (III) reaction of NO_2 and the activated hydrocarbon leading to the formation of N_2 via N-containing organic intermediates. In this regard, there have been a number of studies to promote the NO

reduction activity by combining catalytic active species accelerating certain reaction steps mentioned above. For example, Hamada et al. [6] investigated Co-supported Al_2O_3 catalyst for the selective reduction of NO with propene and proposed a mechanism that the supported cobalt promotes NO oxidation to NO_2, which then reacts with propene on Al_2O_3 to give N_2. Misono et al. [7] reported that the physical mixing of Mn_2O_3 or CeO_2 enhanced considerably the activity of Ce–ZSM-5 for the selective reduction of NO with propene and that the role of Mn_2O_3 or CeO_2 is to promote NO oxidation to NO_2 without accelerating propene combustion.

Recently, non-thermal plasma assisted catalysis is attracting attention as a promising strategy for NOx abatement in diesel exhaust [8]. In this reaction system, the exhaust gas is first treated by a plasma reactor before entering the catalytic converter. In the plasma reactor, NO is oxidized to NO_2 and the hydrocarbons to oxygenates. NO_2 and the oxygenates thus formed then react over the catalyst to produce N_2, CO_2 and H_2O. Since the formation rate of NO_2 and oxygenates can be controlled by adjusting the power for plasma generation, the development of effective catalysts for the reduction of NO_2 with oxygenate under oxygen-rich conditions is highly desirable from a practical point of view.

---

* Corresponding author. Tel.: +81 29 861 9398; fax: +81 29 861 4647.
E-mail address: at-takahashi@aist.go.jp (A. Takahashi).

Kung and co-workers [9] investigated the reaction of NO_2 with CH_3CHO, and found that anatase TiO_2 shows good activity for this reaction. Yoon et al. [10] investigated the activity of various catalysts in the system of plasma-assisted NOx reduction, and reported that Al_2O_3 and basic zeolites such as NaY are effective catalysts. Miessner et al. [11] showed that Al_2O_3 and ZrO_2 act as effective catalysts in plasma-assisted NOx reduction. Tran et al. [12] also reported the activity of In/Al_2O_3, which strongly depends on the type of hydrocarbon used and reaction temperature. However, there have been no comprehensive studies aiming at the development of effective catalyst for plasma-assisted NOx reduction.

In the present study, we have investigated the activity of various alumina-supported catalysts for the selective reduction of NO_2 with CH_3CHO, which are major oxidation products by plasma reaction [13,14], and found that Co/Al_2O_3 shows the highest activity for this reaction. The role of supported Co and the reaction mechanism are discussed based on the catalytic activities for several unit reactions and the behavior of the adsorbed species observed by in situ FT-IR spectroscopy.

2. Experimental

2.1. Catalyst preparation

Alumina supplied from Mizusawa Chemical Industries (Neobead GB-45, $185\,cm^2\,g^{-1}$) was used as the support for catalyst preparation. Alumina-supported catalysts (M/Al_2O_3: M = Mn, Co, Ni, In, Sn, Ga, Ag, Rh) were prepared by impregnation method using aqueous solutions of $Mn(NO_3)_2$, $(CH_3COO)_2Co$, $Ni(NO_3)_2$, $In(NO_3)_3$, $SnCl_4$, $Ga(NO_3)_3$, $AgNO_3$ and $Rh(NO_3)_3$, respectively, followed by drying at $110\,°C$ and calcination in air at $600\,°C$ for 5 h. The loading of metals was set at 1 wt.% except for Co, in which case the loading was changed from 0.5 to 10 wt.%.

2.2. Catalytic activity measurements

The catalytic activity was measured using a fixed bed flow reactor. A 40 mg of a catalyst grinded to powder was placed in the quartz tube. The reaction gas mixture consisting of 500 ppm NO_2, 1500 ppm CH_3CHO, 10% O_2, 6% H_2O and He balance

was passed through the reactor at a gas flow rate of $90\,cm^3\,min^{-1}$ (W/F = $0.027\,g\,s\,cm^{-3}$). Steady-state catalytic activity at each reaction temperature was measured as the reaction temperature was lowered from 600 to 200 °C with a step of 50 °C.

The effluent gas was analyzed by gas chromatography (Shimadzu, GC-8A TCD detector) with a Molecular Sieve 5A column to separate N_2 and CO and a Porapak Q column to separate N_2O and CO_2. The catalytic activity was evaluated in terms of NO_2 conversion to N_2 and that of CH_3CHO to COx (CO + CO_2). The formation of N_2O was found negligible in the present study. The concentration of NOx (NO + NO_2) was continuously monitored with a chemiluminescence NOx analyzer (Shimadzu, NOA-7000) to check the stability of catalytic activity.

2.3. FT-IR measurements

Diffuse reflectance FT-IR spectra were recorded with a Nicolet Nexus 670 FT-IR spectrometer, accumulating 64 scans at a resolution of $4\,cm^{-1}$. Prior to each measurement, 25 mg of a catalyst placed in the diffuse reflectance high temperature cell (Spectra Tech) fitted with CaF_2 windows was activated in situ by heating in flowing 10% O_2/He at 600 °C, followed by cooling to the desired temperature (300–400 °C). The background spectrum of the clean surface was measured for spectra correction. Various gas mixtures containing 0 or 500 ppm NO_2, 1500 ppm CH_3CHO, 10% O_2 and He as the balance gas were fed to the catalyst at a flow rate of $30\,cm^3\,min^{-1}$.

3. Results and discussion

3.1. Activity of alumina-supported catalysts

Table 1 summarizes the catalytic activity of M/Al_2O_3 (M = Mn, Co, Ni, In, Sn, Ga, Ag, Rh) for the selective reduction of NO_2 with CH_3CHO. Al_2O_3 was found to catalyze effectively NO_2 reduction at temperatures above 300 °C with a maximum NO_2 conversion of 46% at 550 °C. It can be seen that Co, Ni, In, Sn, Ga and Ag/Al_2O_3 catalysts showed higher activity than Al_2O_3 with lower effective temperature range. On the other hand, the addition of Mn and Rh caused a significant decrease of the activity of Al_2O_3. The low reduction activity of Mn/Al_2O_3

Table 1
Catalytic activity of Metal/Al_2O_3 for selective reduction of NO_2 with CH_3CHO

Catalysts	NO$_2$ to N$_2$ conversion (%), CH$_3$CHO to COx conversion (%)								
	200°C	250 °C	300 °C	350 °C	400 °C	450 °C	500 °C	550 °C	600 °C
Al_2O_3	0 (0)	1 (4)	13 (15)	21 (33)	27 (59)	42 (83)	43 (91)	46 (99)	29 (96)
Mn/Al_2O_3	0 (6)	0 (18)	0 (28)	0 (45)	0 (77)	9 (95)	11 (97)	10 (99)	7 (99)
Co/Al_2O_3	0 (0)	1 (4)	11 (13)	37 (36)	55 (62)	73 (90)	72 (98)	58 (98)	29 (98)
Ni/Al_2O_3	0 (1)	1 (3)	8 (11)	25 (26)	40 (54)	51 (75)	55 (89)	50 (96)	25 (100)
In/Al_2O_3	1 (0)	1 (3)	10 (10)	28 (27)	49 (63)	55 (86)	56 (97)	51 (99)	26 (100)
Sn/Al_2O_3	1 (1)	1 (5)	16 (14)	29 (31)	33 (58)	47 (82)	53 (92)	53 (96)	27 (99)
Ga/Al_2O_3	1 (1)	2 (4)	15 (13)	28 (29)	34 (58)	46 (78)	51 (88)	58 (95)	32 (97)
Ag/Al_2O_3	1 (2)	1 (6)	5 (13)	15 (29)	20 (56)	32 (85)	59 (96)	61 (99)	33 (100)
Rh/Al_2O_3	0 (3)	1 (11)	3 (27)	12 (86)	3 (97)	1 (98)	0 (98)	0 (98)	0 (98)

Loading of metal: 1 wt.%; reaction conditions: 500 ppm NO_2, 10% O_2, 1500 ppm CH_3CHO, 6% H_2O, He balance and W/F = $0.027\,g\,s\,cm^{-3}$.

and Rh/Al_2O_3 can be ascribed to their high activity for CH_3CHO combustion, as can be seen from the CH_3CHO conversions. Among the additives tested here, Co was the best one, since the maximum NO_2 conversion reaches as high as 73% at 450 °C. Consequently, the rest of this paper deals mainly with Co/Al_2O_3.

3.2. Effect of Co loading on the catalytic activity of Co/Al_2O_3

Fig. 1 shows the effect of Co loading on the catalytic activity of Co/Al_2O_3 for NO_2 reduction with CH_3CHO. NO_2 conversion over Co/Al_2O_3 increased with increasing Co loading and reached a maximum (75%) at 2 wt.% Co loading. However, further increase in the Co loading more than 5 wt.% decreased the NO_2 reduction activity. In contrast, the conversion of CH_3CHO to COx monotonously increased with Co loading. Accordingly, the decrease of NO_2 reduction activity at high Co loading can be explained by predominant CH_3CHO combustion. It was also found that the effective temperature window showing high
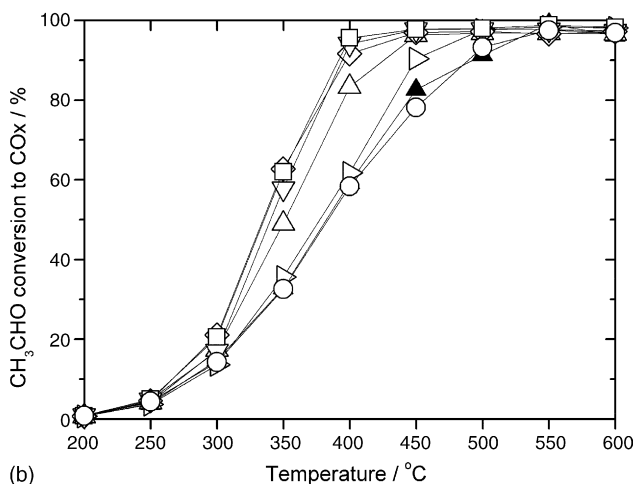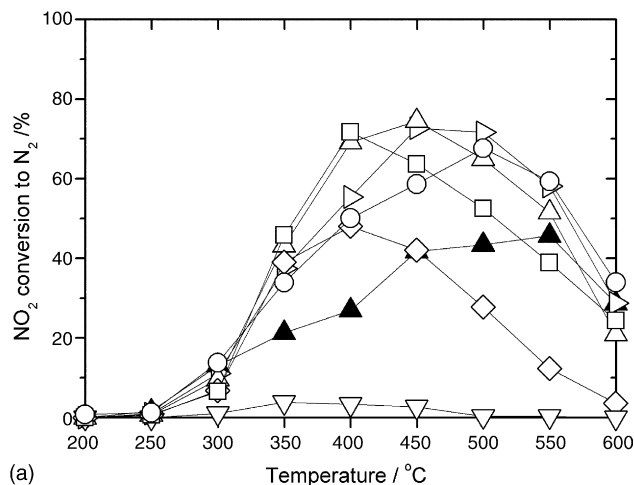

Fig. 1. Effect of Co loading on the catalytic activity of Co/Al_2O_3 for the selective reduction of NO_2 with CH_3CHO. Reaction conditions: 500 ppm NO_2, 10% O_2, 1500 ppm CH_3CHO, 6% H_2O, He balance and W/F = 0.027 g s cm^{-3}. Co loading: 0 wt.% (▲), 0.5 wt.% (○), 1 wt.% (▷), 2 wt.% (△), 3 wt.% (□), 5 wt.% (◇) and 10 wt.% (▽).
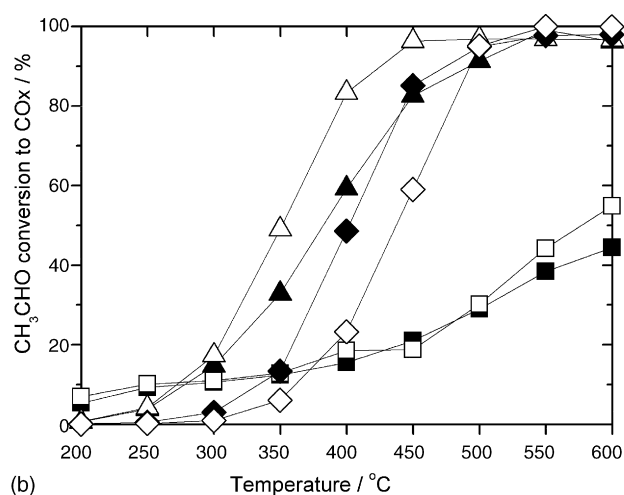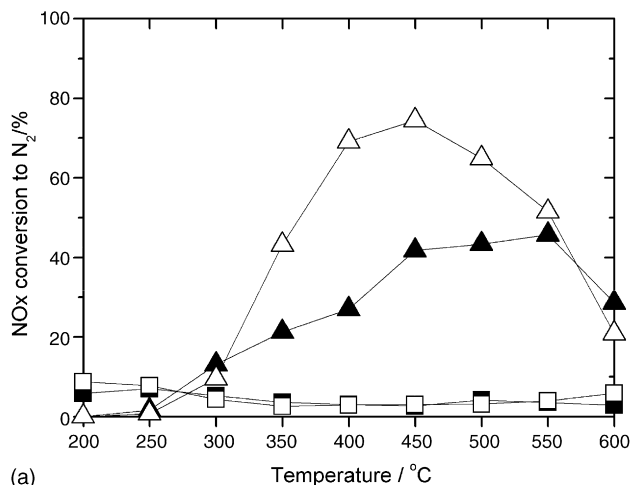

Fig. 2. (a) NO_2 conversion and (b) CH_3CHO conversion for the reaction systems of $NO_2 + CH_3CHO$ (□, ■), $CH_3CHO + O_2$ (◇, ◆) and $NO_2 + CH_3CHO + O_2$ (△, ▲). Open symbols indicated the results obtained on 2 wt.% Co/Al_2O_3 and the solid symbol on Al_2O_3. Reaction conditions: 0 or 500 ppm NO_2, 0 or 10% O_2, 0 or 1500 ppm CH_3CHO, 6% H_2O, He balance and W/F = 0.027 g s cm^{-3}.

NO_2 conversion shifts to lower temperature with increasing Co loading.

3.3. Comparison of $NO_2 + CH_3CHO + O_2$, $NO_2 + CH_3CHO$ and $CH_3CHO + O_2$ reactions

In order to get information on the role of supported cobalt and the reaction mechanism, Al_2O_3 and 2 wt.% Co/Al_2O_3 were examined for catalytic activity for the three reaction systems ($NO_2 + CH_3CHO + O_2$, $NO_2 + CH_3CHO$ and $CH_3CHO + O_2$). Fig. 2(a) shows the NO_2 conversion on Al_2O_3 and 2 wt.% Co/Al_2O_3 for the reaction systems of $NO_2 + CH_3CHO + O_2$ and $NO_2 + CH_3CHO$. Obviously, no NO_2 reduction took place in the reaction system of $NO_2 + CH_3CHO$ on both Al_2O_3 and 2 wt.% Co/Al_2O_3. Furthermore, no NOx reduction was observed in an equal mixture of NO and NO_2 and absence of oxygen on Co/Al_2O_3, suggesting that the presence of O_2 is essential for NO_2 reduction to occur. For NO reduction by hydrocarbons, O_2 is believed to act as an oxidant for NO oxidation to NO_2 and
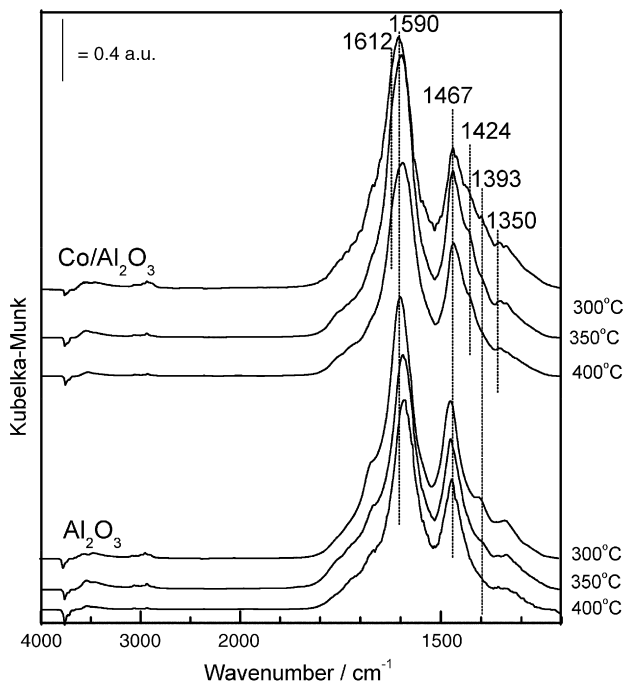
Fig. 3. FT-IR spectra of adsorbed species in flowing CH_3CHO (1500 ppm) + O_2 (10%) on Al_2O_3 and 2 wt.% Co/Al_2O_3 at 300, 350 and 400 °C for 60 min.

Fig. 4. FT-IR spectra of adsorbed species in flowing NO_2 (500 ppm) + CH_3CHO (1500 ppm) + O_2 (10%) on Al_2O_3 and 2 wt.% Co/Al_2O_3 at 300, 350 and 400 °C for 60 min.

oxidative hydrocarbon activation. Since NO_2 was used instead of NO in this study, O_2 is considered to contribute to the activation of CH_3CHO.

The reactivity of CH_3CHO with O_2 was then investigated. As seen in Fig. 2(b), the CH_3CHO conversion on 2 wt.% Co/Al_2O_3 is lower than that on Al_2O_3 for the reaction system of CH_3CHO + O_2. This indicates that one of the roles of Co is to suppress the combustion of CH_3CHO by O_2, which is a side reaction. The addition of NO_2 to the reaction system of CH_3CHO + O_2 slightly increased the conversion of CH_3CHO on Al_2O_3, while a great increase in the conversion was observed on 2 wt.% Co/Al_2O_3. This result strongly suggests that the presence of Co promotes the reaction of NO_2 with CH_3CHO to give N_2.

3.4. FT-IR study

To get further insight into the role of Co and reaction mechanism, we observed FT-IR spectra of adsorbed species formed on Al_2O_3 and 2 wt.% Co/Al_2O_3 under the reaction conditions of CH_3CHO + O_2 and NO_2 + CH_3CHO + O_2.

3.4.1. Surface species formed in CH_3CHO + O_2 reaction

Fig. 3 shows the IR spectra of the adsorbed species formed on Al_2O_3 and Co/Al_2O_3 after introducing the gas mixture of CH_3CHO + O_2 at each temperature. On Al_2O_3, the formation of formate and acetate species was confirmed at 300 °C by the absorption peaks at 1393 and 1590 cm^{-1} (δ(CH) and ν_{as}(COO$^-$) of formate[15–17]) and 1467 cm^{-1} (ν_s(COO$^-$) of acetate[15–17]), respectively. Weak absorption bands due to acetate and formate species were also observed in the C–H stretching region (2900–3000 cm^{-1}). When the temperature
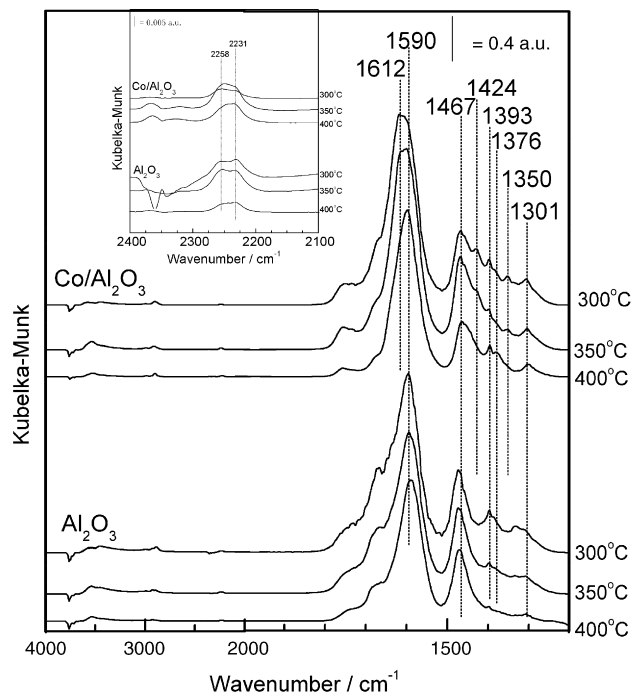
increased up to 400 °C, the bands due to formate species almost completely disappeared, while those due to acetate hardly changed.

In addition to the bands due to formate and acetate described above, new IR bands at 1350, 1424 and 1612 cm^{-1} were detected on Co/Al_2O_3 at 300–400 °C, as can be seen in Fig. 3. The intensities ratio of these peaks was constant though the absolute peak intensities changed about 30% with temperature. Yu et al. [18] observed IR peaks at 1336, 1416 and 1633 cm^{-1} during CH_3CHO oxidation over Ag/Al_2O_3, and assigned them to enolic species(CH_2=CH–O–) on the basis of density functional theory calculation. Theoretical calculations of the vibrational frequencies for enolate (CH_2=C(CH_3)–O) adsorbed on MgO also indicated that the IR bands due to the symmetric and asymmetric stretching vibration of the C–C–O group appear at 1690 and 1426 cm^{-1}, respectively [19]. Therefore, the bands at 1350, 1424 and 1612 cm^{-1} observed here can be assigned to the enolate species (CH_2=CH–O–).

3.4.2. Surface species formed in NO_2 + CH_3CHO + O_2 reaction

The IR spectra measured during the NO_2 + CH_3CHO + O_2 reaction over Al_2O_3 and Co/Al_2O_3 at each temperature are shown in Fig. 4. The IR bands assigned to formate (1376, 1393, 1590 cm^{-1}), acetate (1467 cm^{-1}) and nitrate species (1301 cm^{-1} [17]) were observed on both Al_2O_3 and Co/Al_2O_3 at 300 °C. In addition to these bands, the peaks at 2231 and 2258 cm^{-1} assigned to isocyanate (–NCO) species formed on two different Al^{3+} sites, coordinatively unsaturated tetrahedral and octahedral Al^{3+} [20], respectively, were observed. It should be noted that the bands assigned to enolate species (1350, 1424
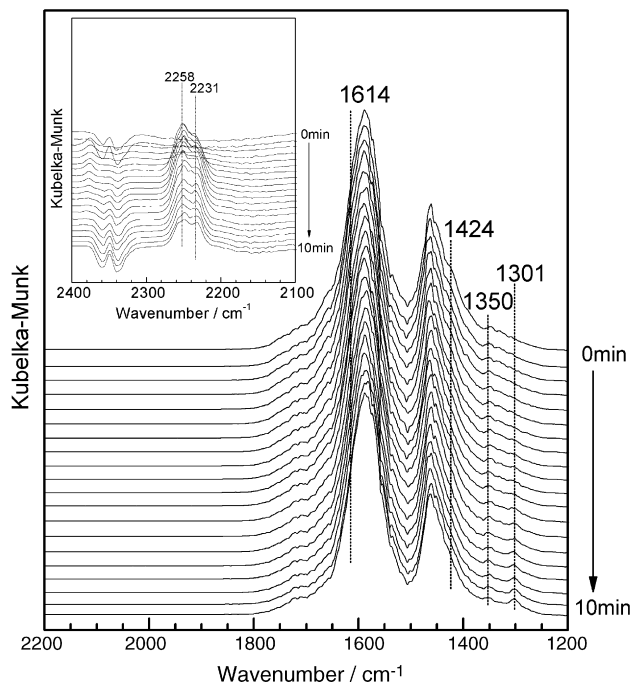
Fig. 5. Change in IR spectra of adsorbed species on 2 wt.% Co/Al$_2$O$_3$ after switching a gas mixture from CH$_3$CHO (1500 ppm) + O$_2$ (10%) to NO$_2$ (500 ppm) + O$_2$ (10%) at 400 °C.

and 1612 cm^{-1}) were detected on Co/Al$_2$O$_3$. Since the enolate species almost completely disappeared at temperatures above 400 °C at which NO$_2$ reduction proceeds (Table 1), this would be an intermediate for NO$_2$ reduction by CH$_3$CHO.

3.5. Reaction pathways of the selective reduction of NO$_2$ with CH$_3$CHO

To confirm the possibility of enolate species as an intermediate, the reactivity of enolate species toward NO$_2$ was evaluated by transient response measurement of IR spectra. The Co/Al$_2$O$_3$ catalyst was first exposed to CH$_3$CHO + O$_2$ for 60 min to accumulate enolate species on the surface, and then the reaction gas mixture was switched to NO$_2$ + O$_2$. This experiment was performed at 400 °C because no formate species, which may react with NO$_2$, existed on the surface at 400 °C (Fig. 3). Fig. 5 shows the change in the IR spectra of adsorbed species after switching the gas mixture to NO$_2$ + O$_2$. It is obvious that the IR band for enolate species decreased and those for nitrate species increased with time on stream. Interestingly, the formation of –NCO species was observed in a few minutes after introducing NO$_2$ + O$_2$. Fig. 6 shows the time dependence of the integrated areas of IR bands due to enolate species (1417–1428 cm^{-1}) and –NCO species (2200–2290 cm^{-1}). Relatively good correlation between the consumption of enolate species and the formation of –NCO species was observed, indicating that the enolate species can react with NO$_2$ to produce –NCO species. Therefore, the enolate species would be an intermediate for NO$_2$ reduction by CH$_3$CHO.

A hypothetical reaction pathway of NO$_2$ reduction by CH$_3$CHO is illustrated in Scheme 1. In the first step, CH$_3$CHO
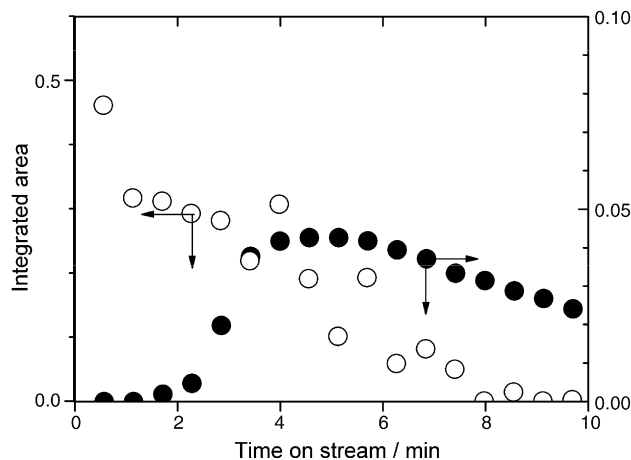

Fig. 6. Time dependence of integrated areas of IR bands due to enolate species (1417–1428 cm^{-1}) (○) and –NCO species (2200–2290 cm^{-1}) (●) on 2 wt.% Co/Al$_2$O$_3$ after switching a gas mixture from CH$_3$CHO (1500 ppm) + O$_2$ (10%) to NO$_2$ (500 ppm) + O$_2$ (10%) at 400 °C.

reacts with O$_2$ to form enolate species. This step would be effectively catalyzed by cobalt sites because the formation of enolate species took place not on Al$_2$O$_3$ but on Co/Al$_2$O$_3$ (Figs. 3 and 4). Some papers reported that the surface enolate species from carbonyl compound such as aldehyde and ketone were formed by the α-hydrogen abstraction of the carbonyl compound, which was proceeded by O^{2-} ions adjacent to cation sites in the cation-anion couple site [21–23]. Ulla et al. showed that Co^{2+} in CoO–MgO solid solution plays a significant role in the formation of O^{2-} species [24]. Co/Al$_2$O$_3$ catalyst is known to contain Co^{2+} incorporated in aluminium oxide lattice in CoAl$_2$O$_4$-like structure [25]. We consider that the O^{2-} ion, which is produced on the sites adjacent to Co^{2+} sites of Co/Al$_2$O$_3$ in the presence of oxygen, abstracts α-hydrogen of acetaldehyde, resulting in the formation of surface enolate. It was reported for hydrocarbon oxidation on transition metal-oxide catalysts that partial oxidation of hydrocarbon effectively occurs on the oxide surface where enolate anion is formed [26]. This is in agreement with the result that the conversion of CH$_3$CHO to COx on Co/Al$_2$O$_3$ was lower than that on Al$_2$O$_3$ during CH$_3$CHO + O$_2$ reaction (Fig. 2). In the second step, the enolate species thus formed reacts with NO$_2$ to give –NCO species (Fig. 5), which is eventually converted to N$_2$. It is known that the nitrosation of enolate by nitrosonium ion (NO$^+$) easily occurs since the enolate is nucleophilic and easily reacts with electrophilic species. It is predicted by ab initio calculation that the nitorosoaldehyde, which is a nitrosation product of CH$_3$CHO via enolate species, easily isomerizes to the glyoxal monoxime, which is an oxime species [27]. Obuchi et al. proposed that –NCO species is formed from organo-nitroso compound via oxime species formation [28].
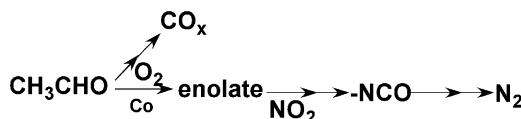
Scheme 1. Proposed reaction pathway for the selective reduction of NO$_2$ with CH$_3$CHO on Co/Al$_2$O$_3$.

Some researchers also reported the transformation of the oxime species to –NCO species [29,30]. Therefore, the possible pathway to –NCO species seems to consist of nitrosation of enolate, isomerization of nitroso species, and transformation of oxime species. In Fig. 5, there is a lag time of about 2 min before NCO band starts to appear, indicating that the induction period is needed for the appearance of the NCO band in the reaction steps from enolate to NCO species. The –NCO species thus formed are rapidly hydrolyzed to NH compounds by reacting with water in the stream and/or on the surface, and then the NH compounds react with NOx species to produce N_2 [29–32]. Because no water was supplied in the FT-IR measurements, the hydrolysis reaction of NCO did not occur and consequently NCO band was still significant while enolate bands have all but disappeared (Fig. 5).

4. Conclusions

Co/Al_2O_3 showed the highest activity for the selective reduction of NO_2 with CH_3CHO of the alumina-supported catalysts tested. The optimum Co loading of Co/Al_2O_3 was 2 wt.%. The comparison of the activity of Co/Al_2O_3 and Al_2O_3 for several unit reactions suggested that one of the roles of supported Co is to suppress the combustion of CH_3CHO by O_2. The observation of the adsorbed species by in situ FT-IR spectroscopy suggested that another role of Co is to promote the production of the enolate species, which is the reaction intermediate leading to N_2 formation.

References

[1] W. Held, A. Koenig, T. Richter, L. Puppe, SAE Paper 900496, 1990.
[2] M. Iwamoto, H. Yahiro, Y. Yu-U, S. Shundo, Y. Yu-U, N. Mizuno, Appl. Catal. 69 (1991) L15.
[3] H. Hamada, Catal. Today 22 (1994) 21.
[4] R. Burch, J.P. Breen, F.C. Meunier, Appl. Catal. B 39 (2002) 283.
[5] M.C. Kung, H.H. Kung, Top. Catal. 28 (2004) 105.
[6] H. Hamada, Y. Kintaichi, M. Inaba, M. Tabata, T. Yoshinari, H. Tsuchida, Catal. Today 29 (1996) 53.
[7] M. Misono, Y. Hirao, C. Yokoyama, Catal. Today 38 (1997) 157.
[8] R.G. Tonkyn, S.E. Barlow, J.W. Hoard, Appl. Catal. B 40 (2003) 207.
[9] A.P. Kozlova, H.-Y. Law, M.C. Kung, H.H. Kung, Catal. Lett. 95 (2004) 211.
[10] S. Yoon, A.G. Panov, R.G. Tonkyn, A.C. Ebeling, S.E. Barlow, M.L. Balmer, Catal. Today 72 (2002) 243.
[11] H. Miessner, K.-P. Francke, R. Rudolph, Appl. Catal. B 36 (2002) 53.
[12] D.N. Tran, C.L. Aardahl, K.G. Rappe, P.W. Park, C.L. Boyer, Appl. Catal. B 48 (2004) 155.
[13] A.G. Panov, R.G. Tonkyn, M.L. Balmer, C.H.F. Peden, A. Malkin, J.W. Hoard, SAE Technical Paper, 2001-01-3513, 2001.
[14] S.J. Schmieg, B.K. Cho, S.H. Oh, SAE Technical Paper, 2001-01-3565, 2001.
[15] M. Haneda, N. Bion, M. Daturi, J. Saussey, J.-C. Lavalley, D. Duprez, H. Hamada, J. Catal. 206 (2002) 114.
[16] F.C. Meunier, V. Zuzaniuk, J.P. Breen, M. Olsson, J.R.H. Ross, Catal. Today 59 (2000) 287.
[17] A. Satuma, K. Shimizu, Prog. Energy Combust. Sci. 29 (2003) 71.
[18] Y. Yu, H. He, Q. Feng, H. Gao, X. Yang, Appl. Catal. B 49 (2004) 159.
[19] J.F. Sanz, J. Oviedo, A. Marquez, J.A. Odriozola, M. Montes, Angew. Chem. Int. Ed. 38 (1999) 506.
[20] N. Bion, J. Saussey, C. Hedouin, T. Seguelong, M. Daturi, Phys. Chem. Chem. Phys. 3 (2001) 4811.
[21] M.I. Zaki, M.A. Hasan, F.A. Al-Sagheer, L. Pasupulety, Langmuir 16 (2000) 430.
[22] M.A. Hasan, M.I. Zaki, L. Pasupulety, Appl. Catal. A 243 (2003) 81.
[23] E. Dumitriu, V. Julea, C. Chelaru, C. Catrinescu, D. Tichit, R. Durand, Appl. Catal. A 178 (1999) 145.
[24] M.A. Ulla, R. Spretz, E. Lombardo, W. Daniel, H. Knozinger, Appl. Catal. B 29 (2001) 217.
[25] T. Maunula, J. Ahola, H. Hamada, Appl. Catal. B 26 (2000) 173.
[26] G. Busca, E. Finocchio, G. Ramis, G. Ricchiardi, Catal. Today 32 (1996) 133.
[27] W.J. Bouma, L. Radom, J. Am. Chem. Soc. 101 (1979) 3487.
[28] A. Obuchi, C. Wögerbauer, R. Köppel, A. Baiker, Appl. Catal. B 19 (1998) 9.
[29] M. Haneda, E. Joubert, J.-C. Ménézoa, D. Duprez, J. Barbier, N. Bion, M. Daturi, J. Saussey, J.-C. Lavalley, H. Hamada, J. Mol. Catal. A 175 (2001) 179.
[30] B.I. Mosqueda-Jimenez, A. Jentys, K. Seshan, J.A. Lercher, Appl. Catal. B 46 (2003) 189.
[31] T. Nanba, A. Obuchi, Y. Sugiura, C. Kouno, J. Uchisawa, S. Kushiyama, J. Catal. 211 (2002) 53.
[32] V. Zuzaniuk, F.C. Meunier, J.R.H. Ross, J. Catal. 202 (2001) 340.